PCCP

Computational predictions on Brønsted acidic ionic liquid catalyzed carbon dioxide conversion to five-membered heterocyclic carbonyl derivatives

Journal:	*Physical Chemistry Chemical Physics*
Manuscript ID	CP-ART-12-2022-005877.R1
Article Type:	Paper
Date Submitted by the Author:	27-Jan-2023

Complete List of Authors:	Abdullayev, Yusif; Baku Engineering University (Former Qafqaz University), Chemical Engineering Department; Institute of Petrochemical Processes, #24 lab Karimova, Nazani; Baku Engineering University, Department of Chemical Engineering Schenberg, Leonardo A.; University of Sao Paulo, Department of Fundamental Chemistry Institute of Chemistry Ducati, Lucas; University of Sao Paulo, Department of Fundamental Chemistry Autschbach, Jochen; University at Buffalo, State University of New York, Chemistry

SCHOLARONE™
Manuscripts

ARTICLE

Computational predictions on Brønsted acidic ionic liquid catalyzed carbon dioxide conversion to five-membered heterocyclic carbonyl derivatives

Yusif Abdullayev[a, b]*, Nazani Karimova[a], Leonardo A. Schenberg[c], Lucas C. Ducati[c] and Jochen Autschbach[d]

Keywords: CO_2 conversion, DFT, molecular dynamics, ionic liquid, energy barriers

Abstract: Experimentally conducted reactions between CO_2 and various substrates (i.e., ethylenediamine (EDA), ethanolamine (ETA), ethylene glycol (EG), mercaptoethanol (ME), and ethylene dithiol (EDT)) are considered in a computational study. The reactions were previously conducted in harsh conditions utilizing toxic metal catalysts (Scheme 1). We computationally utilize Brønsted acidic ionic liquid (IL) $[Et_2NH_2]HSO_4$ as a catalyst aiming to investigate and propose 'greener' pathways for future experimental studies. Computations show that EDA is the best to fixate CO_2 among the tested substrates: The nucleophilic EDA attack on CO_2 is calculated to have a very small energy barrier to overcome (**TS1**$_{EDA}$, $\Delta G^{\ddagger}$=1.4 kcal/mol) and form **I1**$_{EDA}$ (carbamic acid adduct). The formed intermediate is converted to cyclic urea (**P**$_{EDA}$, imidazolidin-2-one) via ring closure and dehydration concerted transition state (**TS2**$_{EDA}$, $\Delta G^{\ddagger}$=32.8 kcal/mol). Solvation model analysis demonstrates that nonpolar solvents (hexane, THF) are better for fixing CO_2 with EDA. Attaching electron donating and withdrawing groups to EDA does not reduce the energy barriers. Modifying IL via changing the anion part (HSO_4^-) central S atom with 6 A and 5 A group elements (Se, P, and As) show that Se-based IL can be utilized for the same purpose. Molecular dynamics (MD) simulations reveal that the IL ion pairs can hold substrate and CO_2 molecules via noncovalent interactions to ease nucleophilic attack on CO_2.

Received 00th January 20xx,
Accepted 00th January 20xx

DOI: 10.1039/x0xx00000x

1. Introduction

Extensive emissions of CO_2 due to anthropogenic factors resulted in rising CO_2 levels in the atmosphere, which causes adverse climate change (e.g., temperature rise, sea-level elevation, and wildfires). Therefore, it is very urgent to tackle the CO_2 emission. Scientists have done intensive research on CO_2 sequestration so far[1, 2]. CO_2 capture and storage (CCS) and CO_2 conversion (CC) to value-added organic compounds were studied[3, 4]. CC is more valuable than CCS because it not only captures CO_2 but also fixates CO_2 into useful multipurpose chemicals. Ethylenediamine (EDA) and its derivatives were used as CO_2 scavengers to produce cyclic ureas.[5-7] Aminoalcohols, i.e., ethanolamine (ETA) and related structures, were employed to fixate CO_2 for the production of oxazolidinones.[8-11] 1,2-diols were utilized for converting CO_2 to cyclic carbonates.[12-15] 1,2-aminothiols were selected to convert CO_2 to thiazolones.[16-19] The aforementioned literature shows that pressurized CO_2 was employed with -NH_2, -OH, -SH functional groups bearing vicinal ethane derivatives in the presence of expensive bases, and cerium (IV) oxide, which is expensive and has toxic effects in human lungs.[20, 21] Organotin compounds utilized in ref. [15] were also found highly neurotoxic.[22] The conditions of the studied reactions need improvement via a 'green' approach: A low-cost and non-toxic catalyst development is vital for CC because of the environmental concerns. Because of the urgent requirement for atmospheric CO_2 level reduction and high industrial demand to the cyclic carbonates, ureas, thiocarbonates, and 2-dithiolone (heterocyclic carbonyl derivatives, HCD) as a solvent, reagent, and monomers, the work is attractive, which inspired us to perform detailed computational studies on the target reactions of Scheme 1.

Ionic liquid (IL)-promoted reactions were utilized in synthetic applications because of the low vapor pressure, high boiling point, recyclability, and low cost of ILs.[23-26].

Density functional theory (DFT) has long been successfully employed to investigate reaction mechanisms.[27-29] CO_2 fixation via various homogeneous catalysts has also become a focus of computational scientists.[30-32] Hwang et al. conducted theoretical

[a] *Department of Chemical Engineering, Baku Engineering University, Hasan Aliyev str. 120, Baku, Absheron, AZ0101, Azerbaijan.*
[b] *Institute of Petrochemical Processes, Azerbaijan National Academy of Sciences, Hojaly ave. 30, Baku, AZ1025, Azerbaijan.*
[c] *Department of Fundamental Chemistry Institute of Chemistry, University of São Paulo Av. Prof. Lineu Prestes, 748 05508-000, São Paulo, SP, Brazil.*
[d] *Department of Chemistry, University at Buffalo, State University of New York, Buffalo, NY 14260-3000, United States.*
† Electronic Supplementary Information (ESI) available: See DOI: 10.1039/x0xx00000x

 This journal is © The Royal Society of Chemistry 2023

studies on the 2-pyrolidone promoted EDA and CO_2 conversion to cyclic urea (imidazolidin-2-one).[5]

In the current work, homogeneous catalytic Brønsted IL-catalyzed CC chemistry is proposed based on quantum chemical calculations, by utilizing EDA, ETA, EG, ME, and EDT as a substrate according to Scheme 1. $[Et_2NH_2]HSO_4$ was taken as a catalyst in this work because of its unique catalytic performance revealed in our previous works.[23, 24] Sulfur atom at the anion component of IL was also replaced with V A and VI A group elements (P, As, and Se) to examine three additional variations of IL on the CC reaction profile. Computational screening of various modifications of ILs on the CO_2+EDA cyclization reaction showed that selenium ($[Et_2NH_2]HSeO_4$) and phosphorus ($[Et_2NH_2]H_2PO_4$) variants should also be tested experimentally for CC reaction with the substrates used in the calculations.

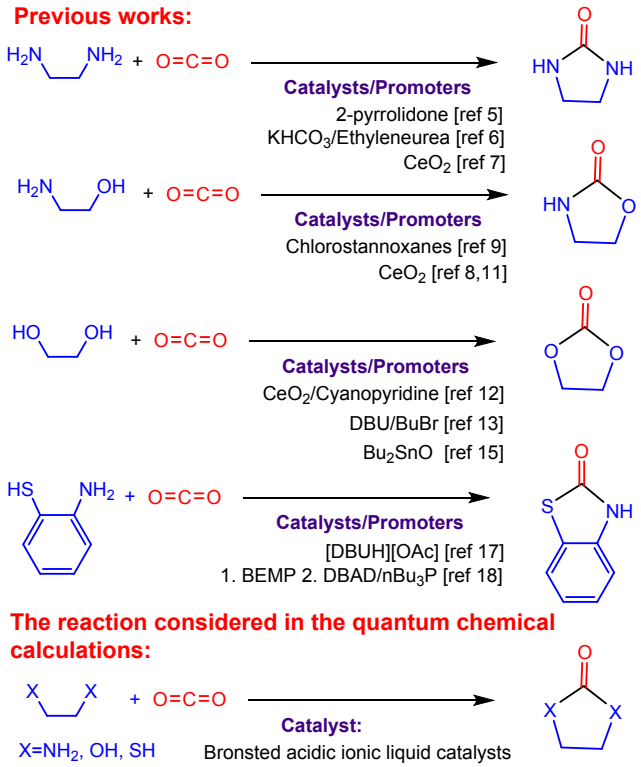

Scheme 1. Screening of previous CC reactions and computationally investigated target CC reactions in the current work.

2. Computational methods

The Gaussian 16 software was utilized for all quantum chemistry calculations.[33] Reactants, intermediates, and transition state structures were optimized with DFT, employing the M062X functional [34] because of its successful application in previous calculations of IL-containing species.[35, 36] 6-31G* basis sets were used for H, C, N, O, S, Se, and P atoms.[37] Solvent effects were studied via a self-consistent reaction field (SCRF), utilizing nonpolar and polar solvents [n-hexane (ε=1.8819), tetrahydrofuran (THF, ε=7.4257), methanol (ε=32.613), and acetonitrile (ε=35.688)]. Minima on the potential energy surfaces (no imaginary frequency) and saddle points (one imaginary frequency mode) at 298.15 K were identified. An intrinsic reaction coordinate (IRC) search was applied to validate the obtained transition states (TSs) associated with intermediate structures. For observing temperature effects on the EDA+CO_2 cyclization reaction, the calculations were performed initially at three different temperatures (298.15, 333.15, and 393.15 K) in a solvent-free condition and 1 atm. High temperature is not influence the Gibbs energy barriers considerably, so further calculations were conducted at 298.15 K. See electronic supporting information (ESI), Figure S1. All the intermediate and TS structures were optimized without geometry constraints. The Cartesian coordinates, total energies, Gibbs energies, and enthalpies are provided in the ESI. Natural bond orbital (NBO) analysis was conducted with the NBO code included with G16, to quantify atomic charges.[38]

An MD simulation of a system containing one molecule of CO_2, one EDA molecule, and 256 ionic pairs of $[Et_2NH_2]HSO_4$ was performed employing the GROMACS package (version 5.1.5).[39] The density of the system was approximated as 1.31 g/mL because Chhotaray et al. calculated this density for similar IL $[HO(CH_2)_3NH_3]CH_3COO$ at 298.15K.[40] Therefore, a cubic box of 38.21 Å was set up to contain the molecules.

The MD has several stages: minimization, equilibration, and production. The minimization stage aims to change the initial positions of the atoms to minimize the energy of the system, and the steepest descent algorithm was adopted. The equilibration stage follows, using the leap-frog algorithm to integrate Newton's equations of motion. This stage occurs in the NVT ensemble with steps of 1 fs. Production MD lasted for a duration of 20 ns. The OPLS-AA was used with parameters provided from the LigParGen server.[41] Atomic charges used in MD simulations were calculated according to the literature.[42]

3. Results and discussion

Calculations show that two TSs are required to reach HCD; the first CO_2 binding step (CB) to the substrate requires lower energy than the ring closure/dehydration concerted step (RCD). The RCD step is a crucial rate-limiting step for HCD formation. CC reaction was first studied with EDA because of its high nucleophilicity relative to other tested substrates. The free energy profile and the related mechanism were designed for EDA+CO_2 reaction (Figure 1). The CB step is calculated to have a 1.4 kcal/mol energy barrier (**TS1$_{EDA}$**) to form **I2$_{EDA}$** ((2-aminoethyl)carbamic acid). The IL-mediated RCD of **I2$_{EDA}$** is going through a high energy barrier (**TS2$_{EDA}$**, $\Delta G^{\ddagger}$=32.8 kcal/mol) to reach **P$_{EDA}$** (imidazolidin-2-one).

This journal is © The Royal Society of Chemistry 2023

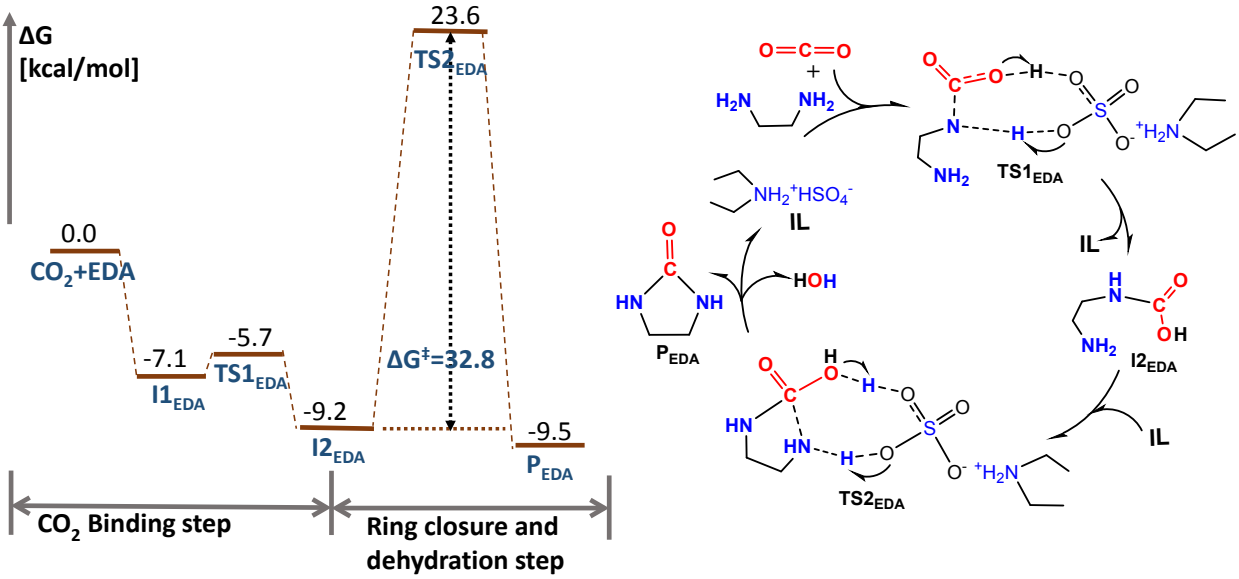

Figure 1. Free energy profile (left) and related calculated mechanism (right) of the IL $(Et_2NH_2]HSO_4$ catalyzed CO_2 conversion to imidazolidin-2-one ($\mathbf{P_{EDA}}$).

Calculations show that EDA binding to CO_2 (1C-1N) is almost barrierless via 1.52 Å distance. Structural analysis of $\mathbf{TS1_{EDA}}$ shows that the anion part (HSO_4^-) of IL ($[Et_2NH_2]HSO_4$) is serving as a proton exchanger via donating its proton to CO_2 (1H-1O, 1.13 Å) and getting proton from the EDA amine group (2H-2O, 1.48 Å) (Figure 2). The $\mathbf{TS2_{EDA}}$ structural analysis shows that the $\mathbf{I2_{EDA}}$ edge primary amine group (2N) attacks the electrophilic carbon (1C, originally the CO_2 carbon) via a 1.62 Å bond distance to form a five-membered ring. The nucleophilic attack facilitates the amine group proton (3H) transfer to the IL HSO_4^- component (3O) via 1.05 Å distance. Simultaneously dehydration over 1C-1O (1.79 Å) bond occurs, which makes $\mathbf{TS2_{EDA}}$ concerted and higher in energy.

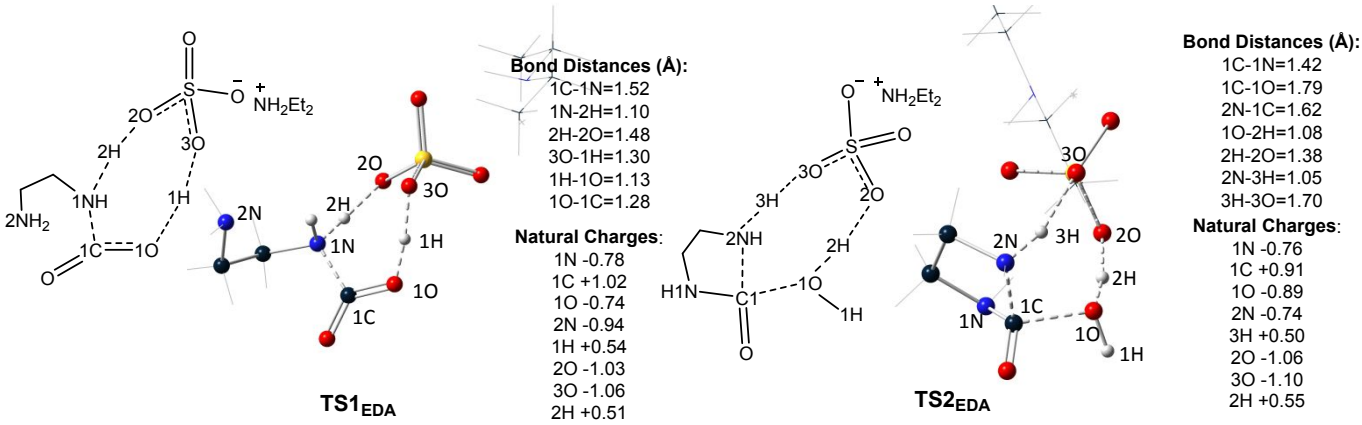

Figure 2. CO_2 binding ($\mathbf{TS1_{EDA}}$) and RCD ($\mathbf{TS2_{EDA}}$) transition states. The IL cation part and some protons are omitted for the sake of clarity.

NBO analysis showed that nucleophilic attack of the EDA nitrogen (1N) on the CO_2 carbon (1C) decreases the electronegativity of 1N (from -0.93 to -0.78) because of the electron density shift toward 1C. Inversely, the CO_2 oxygen (1O, -0.54) electronegativity increases to -0.74 because the C=O π bond electron shift occurs toward 1O simultaneously. The natural charge changes of the other crucial atoms involved in $\mathbf{TS1_{EDA}}$ relative to the original location in substrates and catalyst (EDA, CO_2, and IL) were given in ESI, Table S16.

CO_2 fixation was generally conducted with propylene oxide[43-45] or ethylene oxide[46-48] to produce cyclic carbonates. Our computational studies showed that CO_2 sequestration goes through smaller energy barriers when we utilize other small molecules as a

 This journal is © The Royal Society of Chemistry 2023

substrate. Namely, ethylene oxide was used as a substrate to convert CO_2 for cyclic carbonate in the presence of 1,4,6-triaza-bicyclo[3.3.0]oct-4-enium bromide catalyst.[49] Our computations showed that utilizing EG as a substrate is better since its CB activation Gibbs energy is 10.7 kcal less than the ethylene oxide energy barrier (reported 24.61 kcal/mol). Based on the observation, we can consider additional energy requirements for ethylene oxide ring-opening and poor catalytic performance of the catalyst taken for ethylene oxide+CO_2 conversion as the main influencers to increase energy barriers compared to our case. Zn(salphen) catalyst was used to convert propylene oxide + CO_2 to cyclic carbonates.[50] The CB and RCD steps energy barriers were found to be 48.6 and 66.5 kcal/mol, respectively, for the Zn(salphen) catalyzed CO_2 conversion reaction. The calculated energies are quite high compared to the EG-based CO_2 fixation (See Figure 6). So we propose that the experimentalist utilize the open-chain version of cyclic oxides for CO_2 sequestration.

Substituent effects: Exploiting this scenario (Figure 1), we added different substituents to EDA, viz., -OH, -$N(CH_3)_2$, and -NO_2 to assess substituent effects on the CB and RCD energy barriers (Figure 3). As seen in Figure 3, adding an electron withdrawing group (electron acceptor) or an electron donor group is not facilitating CC. In contrast to EDA route, considerable elevation in energy barriers is observed, e.g., the RDC step when -NO_2 substituted EDA is tested. Because of steric hindrance of Me_2N- group and other factors mentioned below, the CB step energy barrier is significantly higher compared to EDA and other substituted EDA derivatives. Attaching electron donor groups to EDA results in considerable increase on CB energy compared to the unsubstituted EDA CB energy barrier. $\mathbf{TS1}_{\mathbf{HO\text{-}EDA}}$ and $\mathbf{TS1}_{\mathbf{Me2N\text{-}EDA}}$ energies for CB are $\Delta G^{\ddagger}$=6.2 kcal/mol and $\Delta G^{\ddagger}$=11.3 kcal/mol, respectively. We expected electron donors to result in higher nucleophilicity of the EDA amine groups, which may have a smaller energy barrier compared to the calculated CB barriers. The electron density of the EDA amine groups can be polarized toward the electron acceptor (NO_2-)., Accordingly, even higher barriers than those for the electron donors substitution was expected for the CB step was expected. Surprisingly, however, the energy barrier is calculated to be lower for the CB ($\mathbf{TS1}_{\mathbf{NO2\text{-}EDA}}$, $\Delta G^{\ddagger}$=2.5 kcal/mol) step. We visualized the CB and RCD TSs for substituted EDA derivatives to understand the variations of the energy barriers (Figure 4). NBO charge analysis show that in the CB TSs [a) and b), see the figure also regarding the chosen atom numbering] the 1N atom charges are the same as the unsubstituted EDA 1N atom (-0.78), which are (showing the expected electron density shift toward 1N atoms does not occur due to the presence of electron donors. Observations show that 1N atoms in the CB TSs of the unsubstituted, electron donor, and acceptor groups substituted EDA possess the same charge. The CO_2 electrophilic 1C atoms in the related TSs (+1.02), have the same charges also. Therefore, small fluctuations in the CB energy barriers (Figure 3) may be associated with repulsive forces between added substituents and the IL cation and anion components. Additionally, 1C-1N bond distance (1.52 Å) is shorter in $\mathbf{TS1}_{\mathbf{EDA}}$ compared to the same bond in $\mathbf{TS1}_{\mathbf{Me2N\text{-}EDA}}$ and $\mathbf{TS1}_{\mathbf{HO\text{-}EDA}}$, which ease CB considerably via 1.4 kcal/mol energy barrier.

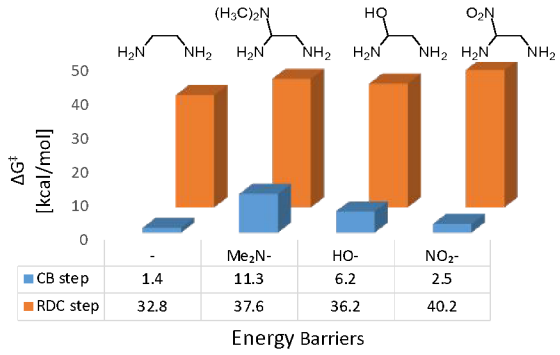

Figure 3. Energy barriers for CB and RCD steps for the EDA derivatives (-OH, -$N(CH_3)_2$, and -NO_2).

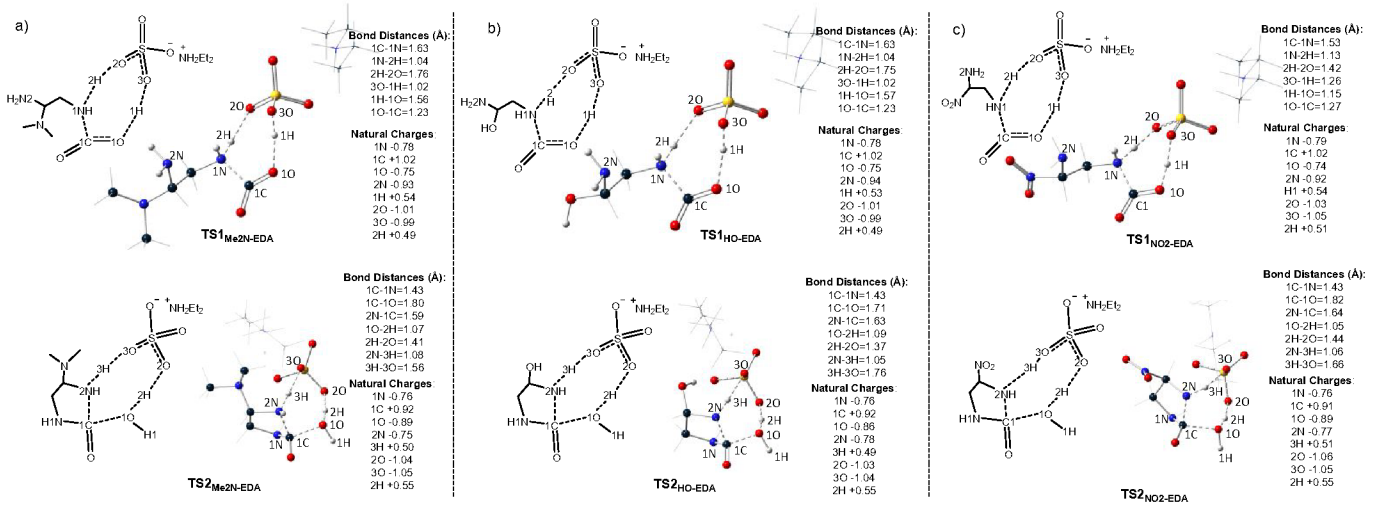

Figure 4. CB and RCD TSs for substituted EDA+CO_2 reaction: a) TSs for Me_2N- substituted EDA, b) TSs for HO- substituted EDA, c) TSs for NO_2- substituted EDA.

This journal is © The Royal Society of Chemistry 2023

Based on the natural charge analysis, it can be suggested that rather than electrophilicity and nucleophilicity of atoms, bond distances can be considered as one of the factors leading to CB energy barriers becoming a little higher in the case of the substituted EDA-based TSs. Calculations show that the tested electron donor and acceptor groups are not capable of influencing the EDA 1N and 2N atomic charges to a substantial degree. Bonds responsible for the RCD (2N-1C, 1C-1O) step, which eventually lead to product formation, may not be considered as a decisive factor to influence energy barriers. Since the interatomic distances do not change considerably as seen from Figure 2 and 4, steric factors are most likely the main influence to increase energy barriers for the RCD step (Figure 3).

Substrate effects: After the analysis of the EDA-based CO_2 fixation, we considered various substrates (ETA, EG, MEA, and EDT) on CO_2 fixation computationally since the substrates were utilized extensively in experimental studies (Scheme 1). According to the free energy profile (Figure 1), EDA was replaced with the aforementioned substrates and energy barriers for CB and RCD steps were calculated for each individual substrate (Figure 5).

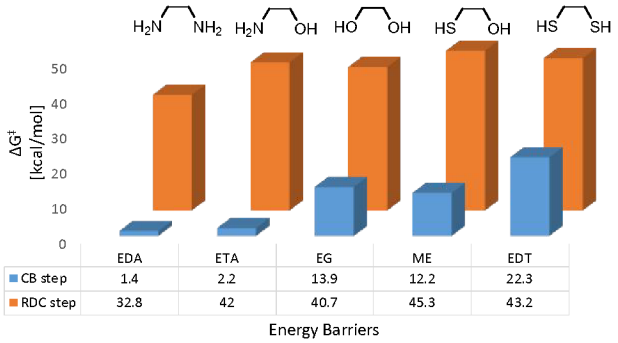

Figure 5. Energy barriers for CO_2 binding and RCD steps for the various substrates (EDA, ETA, EG, ME, and EDT) +CO_2 cyclization to HCD (1 atm, 298.15 K).

The CB step is almost barrierless for EDA and ETA in the presence of the IL catalyst. This is plausible because both substrates are bearing primary amine groups. Unlike EDA, ETA holds hydroxyl and amine functional groups. Primary amine group of ETA is expected to attack first the CO_2 because of its high nucleophilicity. The ETA hydroxyl is a weak nucleophile compared to the amine group, which is a reason why the analogous RCD step for the ETA incorporated step is 9.2 kcal higher than EDA. Examining the EG hydroxyl for the CB step shows that it requires 13.9 kcal energy barrier (the related barrier is calculated to be only 1.4 kcal in the case of EDA). There is no such large energy difference between the ME and EG based CB barriers because the nucleophilic attack to CO_2 is initiated by hydroxyl group. The RCD step energy barrier for the ME based route is 4.6 kcal higher compared to EG because of the weak nucleophilicity of thiol group. The weak nucleophilicity of thiol group is also influences the CB energy barrier (the highest among the tested substrates, 22.3 kcal) for the EDT incorporated cycle.

Based on the calculated energy barriers, EDA was identified as the model substrate for fixating CO_2 (Figure 5). So further optimizations were conducted with only using EDA+CO_2 interactions.

Solvent effects: We tested various solvents via SCRF solvation model on the EDA cycle because of its shallow energy profile (Figure 1). Methanol,[51] THF,[52] acetonitrile,[53] and n-hexane[54] were examined because of their frequent utilization as a solvent in experimental studies related to CO_2 fixation. Solvent polarity is one of the important factors influencing the RCD step. Figure 6 shows that increasing polarity does not affect significantly (ca. ±1 kcal relative to n-hexane) on the CB step (**TS1**$_{EDT}$). Increasing polarity of the employed solvents according to the order: n-hexane < THF < methanol < acetonitrile, increases energy barriers for the RCD steps. The higher polarity may form stronger electrostatic interaction with electrophile (CO_2) adduct, which eventually causes tougher simultaneous RCD (**TS2**$_{EDA}$).

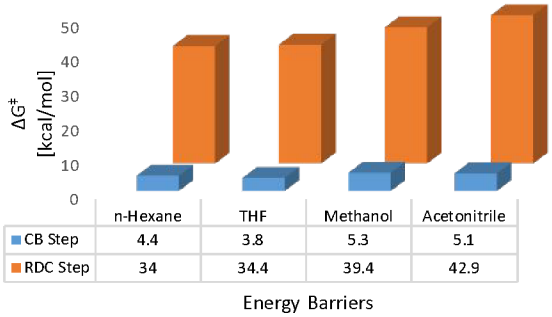

Figure 6. Energy barriers for CO_2 binding and RCD steps for the EDA +CO_2 cyclization to $\mathbf{P}_{EDA}$ exploiting various solvents (n-hexane, THF, acetonitrile, methanol).

Catalyst screening: The model EDA+CO_2 cyclocondensation reaction was tested with different ionic liquid catalysts to show changes on the CB and RCD energy barriers. The IL catalyst anion component central atom was replaced with 5 A, and 6 A group elements (P, As, Se) to design the ILs: $[Et_2NH_2][HSeO_4]$, $[Et_2NH_2][H_2PO_4]$, and $[Et_2NH_2][H_2AsO_4]$ and to examine them on the EDA+CO_2 reaction. Computations show that CB is barrierless and the RCD energy barrier is similar compared to tested IL if Se-based IL is utilized. Replacing sulfur with 5 A group elements such as P and As do not change the RCD energy barrier relative to Se-based IL but significant changes are observed in CB energy barriers as seen in Figure 7. Based on the theoretical investigations it can be suggested that catalytic efficiency of the ILs decreases when 5 A group elements are tested (S→P).

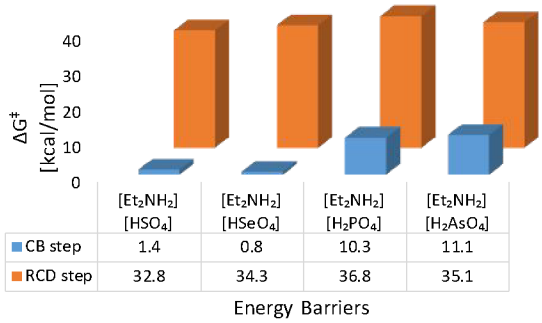

Figure 7. Energy barriers for CO_2 binding and RCD steps for the EDA +CO_2 cyclization to $\mathbf{P}_{EDA}$ in the presence of various IL catalysts ($[Et_2NH_2][HSO_4]$, $[Et_2NH_2][HSeO_4]$, $[Et_2NH_2][H2PO_4]$, and $[Et_2NH_2][H_2AsO_4]$.

This journal is © The Royal Society of Chemistry 2023

MD studies: The cluster analysis tool from GROMACS was used to examine the structure of CO_2 and EDA in 2000 snapshots from the production stage. The largest cluster contains 44 % of the snapshots and the most representative snapshot occurs at time 4120 ps of the dynamic. A representation of this snapshot is presented at Figure 8. MD simulations show that the IL cation and anion pairs play a crucial role in the EDA+CO_2 reaction. As seen from Figure 8 a), the HSO_4^- oxygen atoms form noncovalent interactions with the EDA hydrogen atoms over 2.05 Å distance. Holding both protons with the IL anion pairs increases nucleophilicity of the EDA nitrogen and initiates a nucleophilic attack on the CO_2 electrophilic carbon (3.79 Å). The MD study also suggests that CO_2 is readily available for nucleophilic attack because the IL cation component's methyl protons can form multiple noncovalent interactions (2.65 – 2.85 Å) with the CO_2 oxygen atoms. According to the MD results it can be suggested that taking bulk IL as a medium for the reaction may contribute to the CO_2 fixation process, because of the desired interactions to facilitate a reactive interaction between the substrate and CO_2. Computational studies recommend that the Brønsted acidic ILs desired solvation abilities and catalytic performances make them inevitable systems for CC.

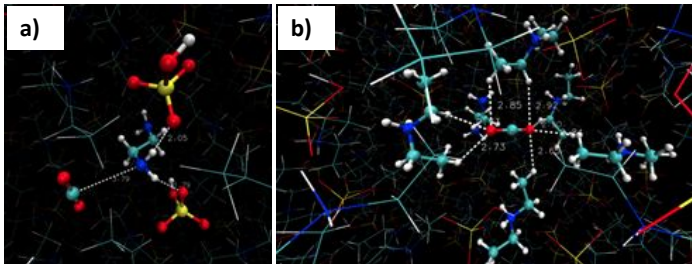

Figure 8. Representation of CO_2 and EDA interaction with the IL anion (HSO_4^-) and cation ($Et_2NH_2^+$) components at the time of 4120 ps of the production stage of MDs and intermolecular interactions length (Å): a) HSO_4^- and EDA interactions b) $Et_2NH_2^+$ and CO_2 interactions.

4. Conclusions

CO_2 fixation utilizing various nucleophilic substances was studied. EDA was utilized first in the quantum chemical calculations because of its higher nucleophilicity relative to other tested substrates. The CO_2 binding to EDA was calculated to have an effectively barrierless (1.4 kcal/mol) step. The next concerted TS rendered cyclic urea formation via ring closure and dehydration (32.8 kcal/mol). Attaching electron donor and acceptor groups to EDA was found to elevate both CB and RCD steps energy barriers because of steric hindrance issues, therefore it was concluded that unsubstituted substrates are more suitable to fixate CO_2 (Figure 3). Theoretical investigations showed that ETA has a similar energy barrier (2.2 kcal/mol) relative to EDA for the CB step since nucleophilic attack was initiated by amine groups in both substrates. In the case of EG and ME substrates, the CB step energy barrier was calculated to be higher, by 13.9 and 12.2 kcal/mol, respectively because of the weak nucleophilicity of -OH compared to -NH_2. Employing EDT was observed to have a twice larger energy barrier (22.3 kcal/mol) for the CB step owing to SH- group compared to the EG and ME substrates. However, no drastic changes for the RCD step energy barriers were found. Our computation suggested EDA utilization to fixate CO_2 is better compared to other examined substrates (Figure 5). Ethylene and propylene oxides were used in the previous experimental studies to fixate CO_2 to cyclic carbonates. Our studies showed that replacing the epoxide ring with related diols, i.e., ethylene oxide with EG, considerably lowers the CB step activation energy for cyclic carbonate formation. MD studies showed that noncovalent interactions between the IL cation component ethyl group protons and the CO_2 oxygen atoms captured CO_2 molecules to ease nucleophilic attack. It was observed that substrate molecule formed noncovalent interaction with the IL anion pairs to increase the -NH_2 group nucleophilicity (Figure 8). Our computational investigations on CC via utilizing substrates generated a map that can help experimentalist to predict how to conduct related experiments.

Conflicts of interest

There are no conflicts to declare

Acknowledgements

Y.A. acknowledges the SOCAR Science Foundation, S/N 12LR-AMEA (05/01/2022) and thanks Isa Valiyev for technical support. L.C.D. and L.A.S. acknowledge grants #2019/18727-0, São Paulo Research Foundation (FAPESP). L.C.D. also acknowledges CNPq #306844/2020-6 grant. J.A. thanks The National Science Foundation, grant CHE-2152633, for support. All authors thank the Center for Computational Research (CCR) at the University at Buffalo for providing computational resources.

Notes

The authors declare no competing financial interest.

References

1. H. A. Patel, J. Byun and C. T. Yavuz, *ChemSusChem*, 2017, **10**, 1303-1317.
2. G. Morello, B. Siritanaratkul, C. F. Megarity and F. A. Armstrong, *ACS Catal.*, 2019, **9**, 11255-11262.
3. Y. Chen and T. Mu, *Green Chem.*, 2019, **21**, 2544-2574.
4. W. Wang, Y. Wen, J. Su, H. Ma, H.-Y. Wang, M. Kurmoo and J.-L. Zuo, *Inorg. Chem.*, 2019, **58**, 16040-16046.
5. J. Hwang, D. Han, J. J. Oh, M. Cheong, H.-J. Koo, J. S. Lee and H. S. Kim, *Adv. Synth. Catal.*, 2019, **361**, 297-306.
6. S.-J. Jin, Y. Khan, J. H. Maeng, Y. J. Kim, J. Hwang, M. Cheong, J. S. Lee and H. S. Kim, *Appl. Catal., B*, 2017, **209**, 139-145.
7. M. Tamura, K. Noro, M. Honda, Y. Nakagawa and K. Tomishige, *Green Chem.*, 2013, **15**, 1567-1577.
8. R. Juárez, P. Concepción, A. Corma and H. García, *Chem. Commun.*, 2010, **46**, 4181-4183.
9. S. Pulla, C. M. Felton, Y. Gartia, P. Ramidi and A. Ghosh, *ACS Sustainable Chem. Eng.*, 2013, **1**, 309-312.
10. S. Zheng, F. Li, J. Liu and C. Xia, *Tetrahedron Lett.*, 2007, **48**, 5883-5886.
11. M. Tamura, M. Honda, K. Noro, Y. Nakagawa and K. Tomishige, *J. Catal.*, 2013, **305**, 191-203.

 This journal is © The Royal Society of Chemistry 2023

12. M. Honda, M. Tamura, K. Nakao, K. Suzuki, Y. Nakagawa and K. Tomishige, *ACS Catal.*, 2014, **4**, 1893-1896.
13. T. Kitamura, Y. Inoue, T. Maeda and J. Oyamada, *Synth. Commun.*, 2016, **46**, 39-45.
14. Y. N. Lim, C. Lee and H.-Y. Jang, *Eur. J. Org. Chem.*, 2014, **2014**, 1823-1826.
15. J. George, Y. Patel, S. M. Pillai and P. Munshi, *J. Mol. Catal. A: Chem.*, 2009, **304**, 1-7.
16. Y. M. Panov, L. V. Erkhova, A. G. Balybin, D. P. Krut'ko and D. A. Lemenovskii, *Russ. J. Phys. Chem. B*, 2019, **13**, 1284-1289.
17. B. Yu, H. Zhang, Y. Zhao, S. Chen, J. Xu, L. Hao and Z. Liu, *ACS Catal.*, 2013, **3**, 2076-2082.
18. K. Horkka, K. Dahl, J. Bergare, C. S. Elmore, C. Halldin and M. Schou, *ChemistrySelect*, 2019, **4**, 1846-1849.
19. J. Paz, C. Pérez-Balado, B. Iglesias and L. Muñoz, *J. Org. Chem.*, 2010, **75**, 3037-3046.
20. D. Schwotzer, H. Ernst, D. Schaudien, H. Kock, G. Pohlmann, C. Dasenbrock and O. Creutzenberg, *Part. Fibre Toxicol.*, 2017, **14**, 23.
21. W. Lin, Y.-w. Huang, X.-D. Zhou and Y. Ma, *Int. J. Toxicol.*, 2006, **25**, 451-457.
22. I. Ferraz da Silva, L. C. Freitas-Lima, J. B. Graceli and L. C. d. M. Rodrigues, *Front. Endocrinol. (Rome, Italy)*, 2018, **8**.
23. Y. Abdullayev, V. Abbasov, L. C. Ducati, A. Talybov and J. Autschbach, *ChemistryOpen*, 2016, **5**, 460-469.
24. I. Valiyev, Y. Abdullayev, S. Yagubova, S. Baybekov, C. Salmanov and J. Autschbach, *J. Mol. Liq.*, 2019, **280**, 410-419.
25. Y. Abdullayev, A. Mammadov, N. Karimova, A. Talybov, U. Yolchuyeva and J. Autschbach, *ChemistrySelect*, 2020, **5**, 6224-6229.
26. A. B. Paninho, A. L. R. Ventura, L. C. Branco, A. J. L. Pombeiro, M. F. C. G. da Silva, M. N. da Ponte, K. T. Mahmudov and A. V. M. Nunes, *J. Supercrit. Fluids*, 2018, **132**, 71-75.
27. H. Xu, K. Muto, J. Yamaguchi, C. Zhao, K. Itami and D. G. Musaev, *J. Am. Chem. Soc.*, 2014, **136**, 14834-14844.
28. Y. Abdullayev, V. Abbasov, F. Nasirov, N. Rzayeva, L. Nasibova and J. Autschbach, *Int. J. Quantum Chem*, e26609.
29. Y. Abdullayev, V. Javadova, I. Valiyev, A. Talybov, C. Salmanov and J. Autschbach, *Ind. Eng. Chem. Res.*, 2022, **61**, 15076-15084.
30. Z. Zhou, B. Qin, S. Li and Y. Sun, *Phys. Chem. Chem. Phys.*, 2021, **23**, 1888-1895.
31. X. Nie, L. Meng, H. Wang, Y. Chen, X. Guo and C. Song, *Phys. Chem. Chem. Phys.*, 2018, **20**, 14694-14707.
32. L. M. Azofra, D. R. MacFarlane and C. Sun, *Phys. Chem. Chem. Phys.*, 2016, **18**, 18507-18514.
33. M. J. Frisch, G. W. Trucks, H. B. Schlegel, G. E. Scuseria, M. A. Robb, J. R. Cheeseman, G. Scalmani, V. Barone, G. A. Petersson, H. Nakatsuji, X. Li, M. Caricato, A. V. Marenich, J. Bloino, B. G. Janesko, R. Gomperts, B. Mennucci, H. P. Hratchian, J. V. Ortiz, A. F. Izmaylov, J. L. Sonnenberg, Williams, F. Ding, F. Lipparini, F. Egidi, J. Goings, B. Peng, A. Petrone, T. Henderson, D. Ranasinghe, V. G. Zakrzewski, J. Gao, N. Rega, G. Zheng, W. Liang, M. Hada, M. Ehara, K. Toyota, R. Fukuda, J. Hasegawa, M. Ishida, T. Nakajima, Y. Honda, O. Kitao, H. Nakai, T. Vreven, K. Throssell, J. A. Montgomery Jr., J. E. Peralta, F. Ogliaro, M. J. Bearpark, J. J. Heyd, E. N. Brothers, K. N. Kudin, V. N. Staroverov, T. A. Keith, R. Kobayashi, J. Normand, K. Raghavachari, A. P. Rendell, J. C. Burant, S. S. Iyengar, J. Tomasi, M. Cossi, J. M. Millam, M. Klene, C. Adamo, R. Cammi, J. W. Ochterski, R. L. Martin, K. Morokuma, O. Farkas, J. B. Foresman and D. J. Fox, Gaussian 16 Rev. A.03, Wallingford, CT2016.
34. Y. Zhao and D. G. Truhlar, *Theor. Chem. Acc.*, 2008, **120**, 215-241.
35. S. Armaković, S. J. Armaković, M. Vraneš, A. Tot and S. Gadžurić, *J. Mol. Liq.*, 2016, **222**, 796-803.
36. D. K. Mishra, B. Banerjee, G. Pugazhenthi and T. Banerjee, *Ind. Eng. Chem. Res.*, 2021, **60**, 9764-9776.
37. R. Ditchfield, W. J. Hehre and J. A. Pople, *J. Chem. Phys.*, 1971, **54**, 724-728.
38. J. P. Foster and F. Weinhold, *J. Am. Chem. Soc.*, 1980, **102**, 7211-7218.
39. M. J. Abraham, T. Murtola, R. Schulz, S. Páll, J. C. Smith, B. Hess and E. Lindahl, *SoftwareX*, 2015, **1-2**, 19-25.
40. P. K. Chhotaray and R. L. Gardas, *J. Chem. Thermodyn.*, 2014, **72**, 117-124.
41. L. S. Dodda, J. Z. Vilseck, J. Tirado-Rives and W. L. Jorgensen, *J. Phys. Chem. B*, 2017, **121**, 3864-3870.
42. A. C. Vendite, T. A. Soares and K. Coutinho, *J. Chem. Inf. Model.*, 2022.
43. T. Wang, D. Zheng, J. Zhang, B. Fan, Y. Ma, T. Ren, L. Wang and J. Zhang, *ACS Sustainable Chem. Eng.*, 2018, **6**, 2574-2582.
44. S. Narang, R. Mehta and S. N. Upadhyay, *Inorganic and Nano-Metal Chemistry*, 2017, **47**, 909-916.
45. X. Hu, P. Wang, W. Liu and Y. Wang, *ChemistrySelect*, 2018, **3**, 6531-6535.
46. J.-Q. Wang, J. Sun, C.-Y. Shi, W.-G. Cheng, X.-P. Zhang and S.-J. Zhang, *Green Chem.*, 2011, **13**, 3213-3217.
47. W. Cheng, Z. Fu, J. Wang, J. Sun and S. Zhang, *Synth. Commun.*, 2012, **42**, 2564-2573.
48. H. S. Kim, J. J. Kim, H. Kim and H. G. Jang, *J. Catal.*, 2003, **220**, 44-46.
49. A. G. Temam and T. A. Lelisho, *Mol. Phys.*, 2020, **118**, 1623931.
50. F. Castro-Gómez, G. Salassa, A. W. Kleij and C. Bo, *Chem. - Eur. J.*, 2013, **19**, 6289-6298.
51. B. M. Bhanage, S.-i. Fujita, Y. Ikushima and M. Arai, *Green Chem.*, 2003, **5**, 340-342.
52. C. Taddei, S. Bongarzone and A. D. Gee, *Chem. - Eur. J.*, 2017, **23**, 7682-7685.
53. N. E. Mendieta-Reyes, W. Cheuquepán, A. Rodes and R. Gómez, *ACS Catal.*, 2020, **10**, 103-113.
54. Q. Liu, X. Yang, L. Li, S. Miao, Y. Li, Y. Li, X. Wang, Y. Huang and T. Zhang, *Nat Commun*, 2017, **8**, 1407.

 This journal is © The Royal Society of Chemistry 2023